November 1998 NREL/CP-520-25654

UV-VIS-IR Spectral Responsivity Measurement System for Solar Cells

H. Field

Presented at the National Center for Photovoltaics Program Review Meeting, September 8–11, 1998, Denver, Colorado

National Renewable Energy Laboratory
1617 Cole Boulevard
Golden, Colorado 80401-3393
A national laboratory of
the U.S. Department of Energy
Managed by Midwest Research Institute
for the U.S. Department of Energy
under Contract No. DE-AC36-83CH10093

Prepared under Task No. PV903401

November 1998

UV-VIS-IR Spectral Responsivity Measurement System for Solar Cells

Halden Field

National Renewable Energy Laboratory (NREL)
1617 Cole Blvd., Golden, Colorado, USA 80401

Abstract. NREL's PV Cell and Module Performance Characterization group has built a new spectral responsivity measurement system for solar cells. It uses a xenon arc lamp source, a single, grating monochrometer, and a fiber-optic bundle to couple the monochromatic light to the test device. The system has a spectral bandwidth of 2 nm, minimum spot diameter of 1.6 mm, a spectral range of 280-1330 nm, and uncertainty better than ±3% over most of this range. It is capable of incorporating light bias with intensities exceeding one sun. This paper discusses the system's features, capabilities, calibration, and measurement uncertainties.

BACKGROUND

A photovoltaic (PV) device's spectral responsivity describes its ability to convert light of various wavelengths to electricity. It is often reported as the ratio of device current divided by incident-beam power (e.g., A/W) or device current divided by incident photon flux (i.e., quantum efficiency). Researchers can use spectral responsivity measurements to help understand device operation. Data from such measurements are also used in spectral mismatch parameter (1) calculations used to set solar simulator intensity for solar cell and module performance measurements.

SYSTEM DESCRIPTION

Figure 1 illustrates the system's major components and their configuration. Table 1 lists major system specifications. Calibration devices are NIST-calibrated silicon photodiodes and a Laser Probe RS-5900 electrically-calibrated pyroelectric radiometer calibrated by the manufacturer with NIST traceability. Other component details are available from the author.

PROCEDURES

To determine a device's spectral responsivity, one must know the power or irradiance reaching the test device at each wavelength and the current produced by the device at each of those wavelengths. In this system, the power is measured with a calibrated photodiode or a pyroelectric radiometer. At the same time, the current produced by the monitor photodiode is measured. The computer controlling the system records the ratio of these two quantities for later use when the test device's response is measured.

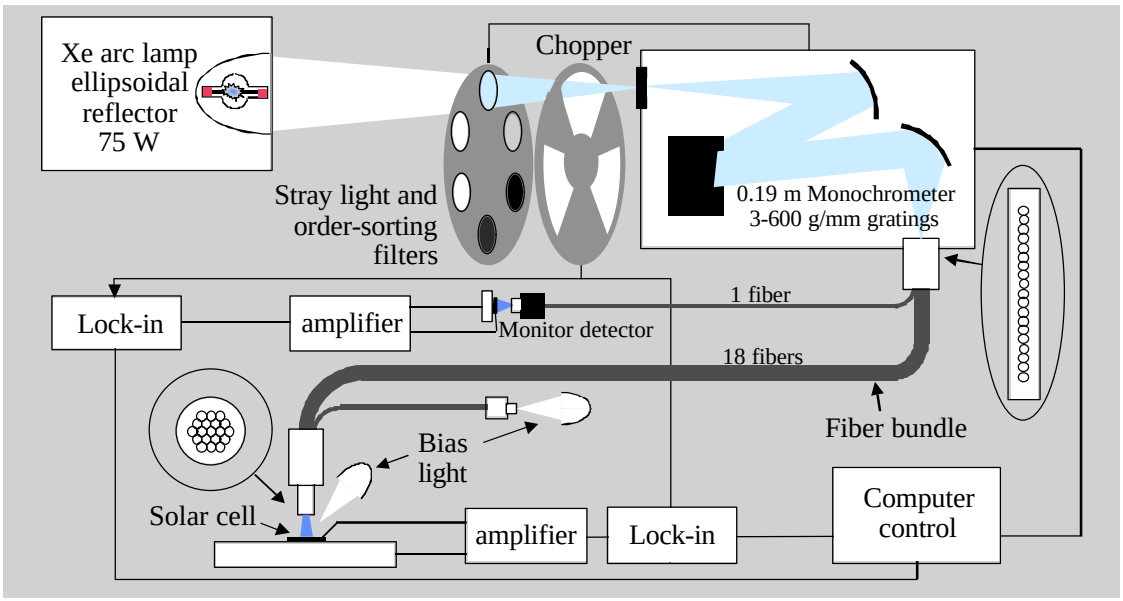

FIGURE 1. Equipment configuration for spectral responsivity measurement system.

TABLE 1. System Specifications

Item	Specification	Notes
Spectral range	280-1330	no light bias
Spectral resolution	2 nm	monochromatic beam spectral bandwidth
Spectral step size	0.14 nm	minimum
Uncertainty	≤3%	310-1060 nm, no light bias
	≤10%	< 310 nm, >1060 nm, no light bias
Wavelength uncertainty	±2 nm	
Beam size	1.6-mm diameter	minimum
Beam power	~80 µW	maximum
Beam power density	~4 mW/cm^2	0.04 "suns"
Light-bias capability	≥ 1.5 "suns"	small or apertured devices

During a test, the computer records the currents produced by the test device and the monitor photodiode at the same time for each wavelength in the test. Using the power-to-current ratio previously recorded, it converts the monitor current to a beam power quantity. The ratio of test device current $I_{TD}(l)$ to beam power is the device responsivity, which is converted to units of quantum efficiency by using the monochrometer's wavelength setting l:

$$QE(l) = \frac{100\% \cdot h \cdot c \cdot I_{TD}(l)}{e \cdot l \cdot I_{MON}(l) \cdot CV_{MON}(l)}, \qquad (1)$$

where h is Planck's constant, c is the speed of light, e is the electron charge, $I_{MON}(l)$ is the monitor-cell current, and $CV_{MON}(l)$ is the monitor cell's calibration value in W/A units.

UNCERTAINTIES

This system estimates the uncertainties in its measurements by quantitatively combining uncertainty estimates from various sources during the measurement procedure. It specifies systematic and random components explicitly in the measurement report.

Table 2 lists the uncertainties considered for this estimation process. The uncertainty introduced during system calibration depends on the reference device used. The pyroelectric radiometer has uncertainty in the factor applied to correct its readings because the chopped waveform is not square, in its electrical–optical equivalence, in its amplifier gain, and in its analog-to-digital converter. The estimate treats as random uncertainties the drift in instrumentation gain during the measurement and the potential gain or detector nonlinearities because they change during the calibration as signal levels vary.

TABLE 2. Uncertainty Estimates

Source	**Bias**	**Random**
Calibration – pyroelectric radiometer	2%	2% + as measured
Calibration – photodiode	0.2-4.4% + 1%	1% + as measured
Measurement	1%	1% + as measured

The photodiode calibration report from NIST (2) provides uncertainty estimates for each wavelength with the spectral responsivity data. The software combines these with an additional estimate to account for other uncertainties, including the effect of multiple light reflections between the photodiode and the beam-delivery optics. Uncertainties are combined with the root-sum-square method for the 95% confidence estimate. Fixed instrumentation-gain errors do not contribute to the total uncertainty, because the same instruments are used to amplify the photodiode and test-device signals.

The computer collects multiple readings from the calibration device and monitor detector at each wavelength and computes the ratio for each reading. It combines the standard deviation of these ratios, multiplied by the appropriate student's *t* factor, with the random-error estimate associated with the calibration device used, to estimate the "as measured" part of the random uncertainty for the calibration shown in Table 2.

The computer combines the bias and random uncertainties in the calibration with an additional uncertainty to include the effects of wavelength uncertainty on the quantum-efficiency calculation, multiple reflections between the test device and the beam-delivery optics, and others. This result is the bias uncertainty estimate for the data report. The program estimates the measurement random uncertainty by the method described above for the calibration's random uncertainty. It combines this with an additional uncertainty to account for potential instrumentation gain-drift and nonlinearity during the test. Figure 2 illustrates the uncertainty of a measurement made using this system.

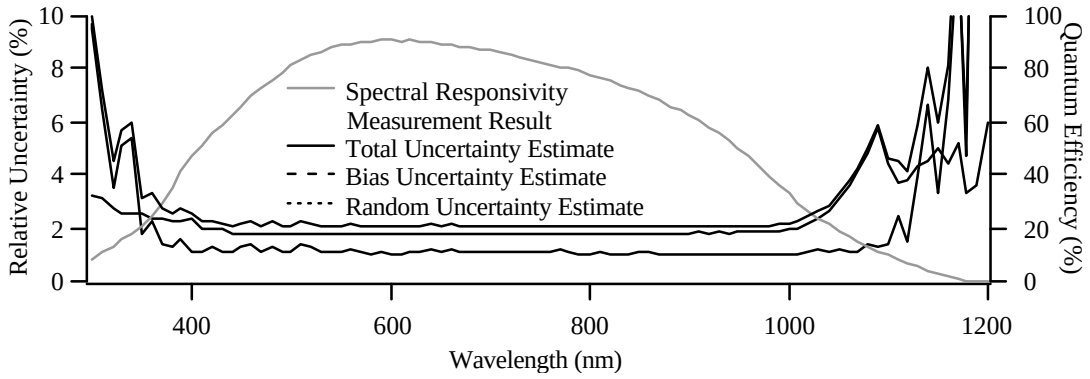

FIGURE 2. Measurement example and uncertainty estimates (24 mA/cm^2 bias light)

WAVELENGTH CALIBRATION AND SPECTRAL BANDWIDTH

Adjusting the monochrometer offsets to minimize the difference between its wavelength settings and the results of wavelength calibration checks provides the system's wavelength calibration. Calibration points are provided by line filters calibrated by NREL's CARY 5G spectrophotometer, xenon arc lamp emission lines (3), and a helium-neon laser.

Narrow-bandpass (~1-nm) filters commonly used to isolate laser wavelengths were placed over a photodiode, and the responsivity of the combination was measured. Filters with center wavelengths of 324.7, 440.7, 514.5, and 633.1 nm produced responsivity peaks within 0.8 nm of the expected wavelength. Emission lines in the system's source at 823.2, 980.0, and 992.3 nm appeared 1.2 to 1.8 nm higher than expected in the current vs. wavelength profiles of a bare photodiode's current. Light from a helium-neon laser aligned with the center of the monochrometer appeared within 0.7 nm of the expected wavelength using first-, second-, and third-order diffractions for all three gratings.

The physical positions of the monochrometer's diffraction grating, its other optical components, and the line of optical fibers simulating its exit slit determine the wavelength of the light that reaches the fiber bundle. The relative positions of these components change with temperature. In addition, position repeatability limits for the grating (the one moving part) affect the wavelength calibration. Optical properties of the gratings and fiber optics can contribute to wavelength errors. Finally, errors in the wavelength calibration sources themselves contribute to wavelength uncertainty. Rather than analytically characterize all of the known, potential error sources, an uncertainty estimate of ±2 nm is assigned to encompass these observations. Wavelength calibration errors can also affect the calculation of device quantum efficiency, as the wavelength enters the conversion from power to photon flux (see Equation 1).

Small wavelength changes can cause large changes in monochromatic beam intensity when the light source has strong emission lines and the monochrometer wavelength is set near one of those lines. The use of a monitor cell in this system enables the measurement to be relatively insensitive to such changes, as the ratio of test-cell and monitor-cell currents is used to determine the test-device responsivity.

With the helium-neon laser used in place of the xenon arc lamp source, the current vs. wavelength profile of a photodiode signal indicates that the system bandwidth is 1.4 nm, consistent with the monochrometer's design specifications. However, similar measurements across xenon emission lines and line filters indicate that the bandwidth may be slightly higher. Though this may be due to finite bandwidth of the line filters and broadening of the emission lines, the system's spectral bandwidth is specified to be ≤2 nm.

CONFIGURATION ISSUES

Light Modulation and Filters

Use of a light chopper with the monochrometer enables the lock-in amplifier to discriminate between the test-device current resulting from monochromatic light and that from stray and bias light. Order-sorting filters attenuate light that would appear at the monochrometer exit because of higher-order diffractions than the intended one. Stray-light filters attenuate light that could reach the monochrometer exit resulting from reflections from the various surfaces inside the monochrometer, including the mirrors and grating themselves.

The light chopper and filter wheel are outside the monochrometer entrance because the presence of the fiber-optic bundle prevents them from being placed at the exit. In this position, the filters reduce the total light reaching the monochrometer, thus reducing heating of the instrument. A disadvantage is that the filters get hot, changing their spectral transmittance. Delays to stabilize filter temperature are incorporated in the software to avoid errors from this problem. Heat can also damage the filters, but a broken filter does not appear to affect this system's performance.

Fiber-Optic Bundle

Common light fibers used for communication have poor transmission in the ultraviolet (UV). This system uses a fiber doped with OH^- ions to boost its UV transmission. A drawback is that the OH^- causes substantial absorption between 1340 and 1410 nm, limiting the system's continuous spectral range. The fiber's numerical aperture of 0.22 enables it to accept most of the light from the f/3.9 monochrometer.

The light fibers are linearly arranged at the bundle entrance to optically resemble a common monochrometer's output slit. Eighteen fibers convey light to the test or calibration device, where the fibers are arranged in a circle. One fiber conveys a sample of the light to the monitor cell, which functions as a calibration transfer standard. One additional fiber can convey light from a bias light source to the test

device (see Figure 1), but this method is not yet sufficiently developed. At present, a projector lamp provides bias light.

Multiple Reflections

Light reflected from the test or calibration device can, in turn, be reflected back to the device by the end of the fiber bundle. Additionally, a small amount of light exits the fiber outside the expected "cone." The effect appears as a dependence of signal magnitude on fiber-to-device distance. To minimize this effect, a painted cap covers the ferrule holding the fibers. The paint's reflectivity is about 4%, with little spectral dependence. Even with these precautions, the signal produced by a relatively high-reflectivity photodiode varies about 1% between fiber-to-device distances of 3 and 12 mm.

BEAM POWER AND STRAY LIGHT

Figure 3 presents the spectral beam power for this system. Signal-to-noise performance and the leakage of low-level, out-of-band light through the filters and monochrometer limit measurement capability where the monochromatic beam power is lowest. Figure 4 shows that stray light is well under control in the UV and infrared regions. The left graph shows the device quantum efficiency reported, with the UV component of the monochromatic beam blocked by a 3-75 colorglass filter. The low signal levels represent the extent that stray light influences the measurement results. The right graph shows the device quantum efficiency reported in wavelength ranges for which the test device (a photodiode) should not respond.

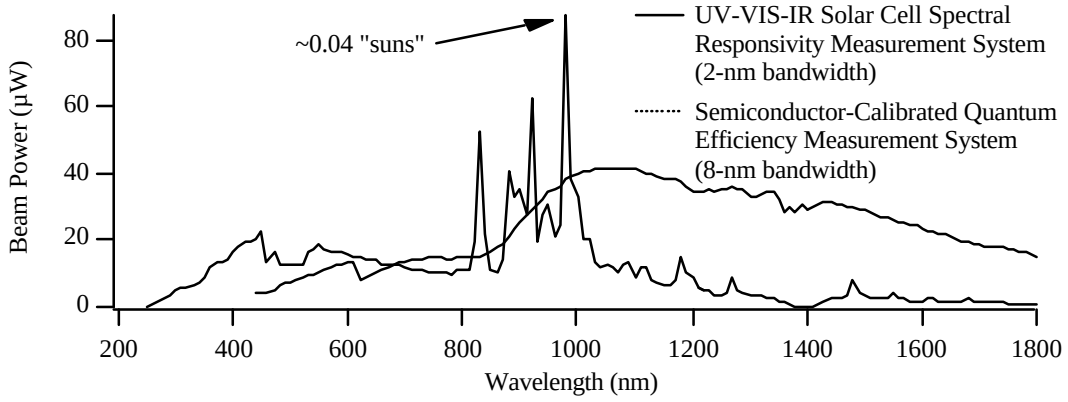

FIGURE 3. This system's beam power is compared to that of another spectral responsivity measurement system at NREL.

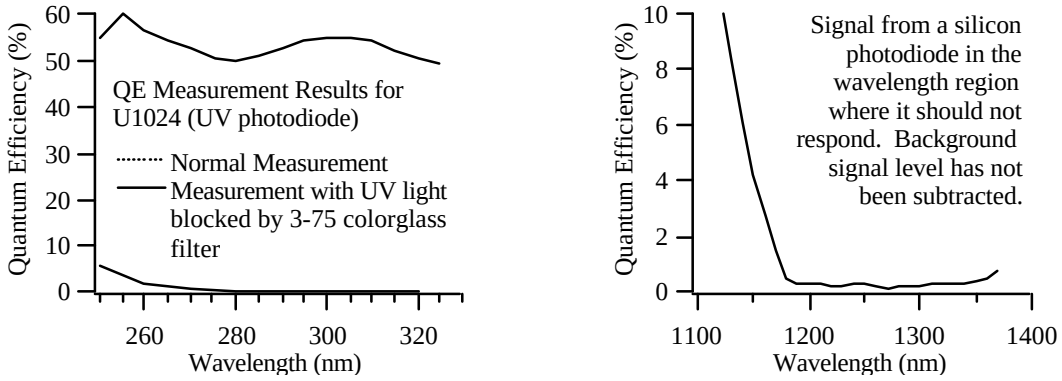

FIGURE 4. These graphs illustrate that stray light is minimal in wavelength regions where it is most likely to be a problem.

FURTHER IMPROVEMENTS

Measurements on this system, performed on request to the author by participants in DOE's PV Program, provide a valuable diversity of device characteristics and configurations, revealing opportunities for the system's continuing development. The author would appreciate feedback from potential measurement requesters on additional ideas for this list and suggestions for how to prioritize these items:

- Substitute rigorous, quantitative analysis for uncertainty judgements.
- Reduce measurement uncertainty.
- Improve wavelength calibration.
- Extend spectral range below 280 nm or above 1330 nm.
- Include uncertainty estimates in measurement reports graphically.
- Add option to measure responsivity in equal eV or wavenumber increments.
- Increase bias-light capability.
- Add temperature control for test devices.

ACKNOWLEDGEMENTS

The author thanks Ramesh Dhere of NREL for spectral transmissivity and spectral reflection measurements used to explore wavelength-calibration and multiple-reflection issues. DOE supported this work under Contract Number DE-AC36-83CH10093.

REFERENCES

1. "Standard Test Method for Determination of the Spectral Mismatch Parameter Between a Photovoltaic Device and a Photovoltaic Reference Cell [Metric]," ASTM Standard E 973M – 96, West Conshohocken, PA: American Society for Testing and Materials, 1996.

2. T.C. Larason, S.S. Bruce, A.C. Parr, *NIST Special Publication 250-41 Spectroradiometric Detector Measurements*, Washington, D.C.: U.S. Government Printing Office, 1998, pp. A-17-19. Also available at http://ois.nist.gov/sdm/

3. Weast, R., Astle, M., and Beyer, W., *CRC Handbook of Chemistry and Physics*, Boca Raton, Florida: CRC Press, Inc., 1983, pp. E-305.